

DISSERTATION

---

**Automated optimization of sensitivity in  
a search for boosted VBF Higgs pair  
production in the  $b\bar{b}b\bar{b}$  quark final state  
with the ATLAS detector**

---

For the attainment of the academic degree doctor rerum naturalium

(Dr. rer. nat.) in the subject: Physics

**Frederic Renner**

Berlin, 07.12.2023

Faculty of Mathematics and Natural Sciences of the Humboldt  
University of Berlin

1st Supervisor: Dr. Clara Elisabeth Leitgeb

2nd Supervisor: Prof. Dr. Cigdem Issever

---

(Only after the disputation for publication in the university library according to § 15 of the doctoral regulations enter the names and the date):

Reviewers:

1st:

2nd:

3rd:

Date of the oral examination:



## Abstract

I am an abstract.



---

# Contents

<b>1</b>	<b>Systematic Uncertainties</b>	<b>1</b>
1.1	Luminosity . . . . .	1
1.2	Jet Uncertainties . . . . .	1
1.3	$X \rightarrow b\bar{b}$ Tagger Uncertainties . . . . .	2
1.4	Theory Uncertainties . . . . .	3
1.4.1	Uncertainty on HH cross section . . . . .	4
1.4.2	Uncertainty on Acceptance . . . . .	4
1.4.3	Parton Shower . . . . .	4
1.4.4	Branching Ratio Uncertainty . . . . .	5
1.5	Statistical Uncertainties . . . . .	5
1.6	Background Derivation Uncertainties . . . . .	6
<b>2</b>	<b>Statistics</b>	<b>7</b>
2.1	Profile Likelihood Ratio . . . . .	7
2.2	Test Statistic and p-value . . . . .	9
2.3	The $\text{CL}_s$ value . . . . .	12
2.4	HistFactory . . . . .	13
2.5	The Modifiers . . . . .	15
2.6	The constraint terms . . . . .	18
<b>I</b>	<b>Results</b>	<b>20</b>
<b>3</b>	<b><math>HH \rightarrow 4b</math> Results</b>	<b>21</b>
3.1	Background validation . . . . .	21

---

Appendices	23
A Acronyms	23
B Cutflow	26
Bibliography	29

---





# Chapter 1

## Systematic Uncertainties

Any measurement needs to consider uncertainties in order to determine its validity. In this analysis they can be divided into systematic errors for the reconstructed objects, uncertainties from theoretical calculations, methodological errors and statistical uncertainties and are described in the following.

### 1.1 Luminosity

The combined integrated luminosity for the years 2015-2018 has an uncertainty of 0.83% determined with the LUCID-2 detector and is applied. It is applied to the Higgs Pair Signal process and has minimal impact on the analysis.

### 1.2 Jet Uncertainties

Jets are calibrated using well known reference objects as described in section ???. These corrections are themselves subject to uncertainties related to detector effects, modeling and statistics leading to corrections of the jet energy and are collectively referred to as Jet Energy Scale (JES) [1, 2]. Since simulations of jets have a higher accuracy than observed jets the uncertainties of the simulated jets are broadened to be consistent with the jets observed in the data. These uncertainties are known as Jet Energy Resolution (JER). Furthermore large- $R$  jets are additionally corrected

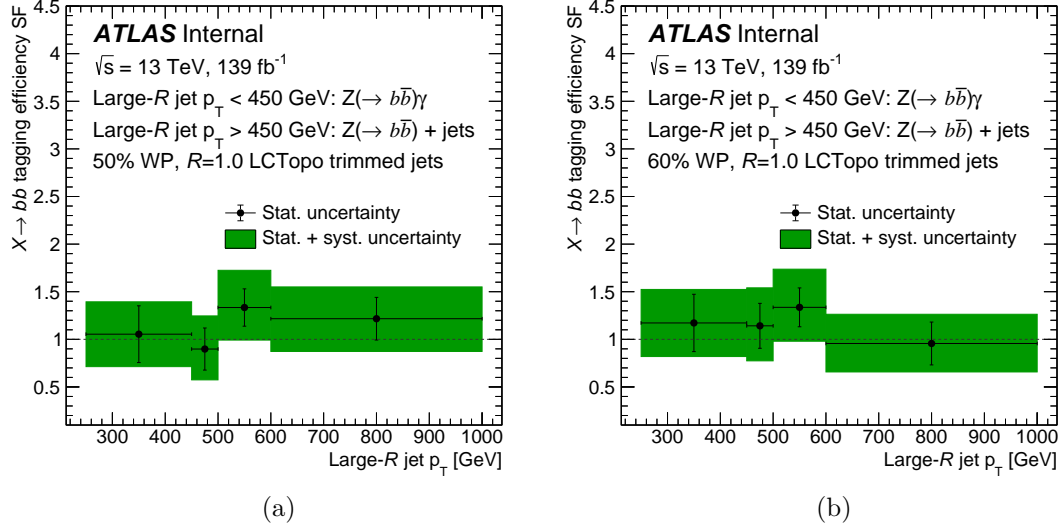


**Figure 1.1:** Derived scale factors in large- $R$  jet  $p_T$  for the (a) 50 % and (b) 60 % working point (WP) from the calibration of the  $X \rightarrow b\bar{b}$  tagger.

for their mass. The uncertainties related to this procedure are called Jet Mass Resolution (JMR) [3].

### 1.3 $X \rightarrow b\bar{b}$ Tagger Uncertainties

The Neural Network (NN) of the  $X \rightarrow b\bar{b}$  tagger was trained using simulations leading to potential discrepancies in selection efficiencies between observed data and simulation. Calibration is conducted with  $Z(\rightarrow b\bar{b}) + \text{jets}$  and  $Z(\rightarrow b\bar{b}) + \gamma$  applying the same methodology as in [4]. However as of this analysis the  $b$ -tagging algorithm for the variable radius (VR) track jets has been updated to the DL1d algorithm described in section ???. The differences between Monte Carlo (MC) and data are measured in large- $R$  jet  $p_T$  and the extracted scale factors and their corresponding combined systematic and statistical uncertainties are shown in figure 1.1.

## 1.4 Theory Uncertainties

The cross-section calculation for some process initiated by a proton proton collision calculated at  $n$ -th order has a functional form [5]

$$\sigma^{(n)} = PDF(x_1, \mu_F) PDF(x_2, \mu_F) \hat{\sigma}^{(n)}(x_1, x_2, \mu_R), \quad (1.4.1)$$

with the Parton Density Functions (PDFs) carrying momentum fraction  $x_{1,2}$  of the partons and the factorization scale  $\mu_F$ . This scale is named after the assumption that the cross-sections of the initial particle can be calculated by factorizing it in its parton contributions [6]. The term  $\hat{\sigma}^{(n)}$  in equation 1.4.1 is the calculable part of the cross-section at renormalization scale  $\mu_R$  as described in section ?? and is expanded to a desired order  $n$  in the strong coupling constant  $\alpha_s$  with the usual Quantum Field Theory (QFT) ansatz outlined in section ??

$$\hat{\sigma}^{(n)} = \alpha_s \hat{\sigma}^{(0)} + \alpha_s^2 \hat{\sigma}^{(1)} + \dots + \alpha_s^n \hat{\sigma}^{(n)} + \mathcal{O}(\alpha_s^{n+1}). \quad (1.4.2)$$

Modelling cross-sections via PDFs is necessary since the approximation of the perturbation ansatz of section ?? breaks down for low energy scales  $Q^2$  as described in section ?? which is the energy scale for which the approximation would need to hold to describe the partons inside a proton. However similar to renormalization a scaling behavior can be derived which allows to deduce an estimate of the PDFs by measuring it at a some energy scale  $Q^2$  to extrapolate it to another. The equations enabling this are also expanded in  $\alpha_s$  to a desired order and are known as DGLAP equations [6]. Three main sources of uncertainty arise in this calculation described in the following.

### Scale Variations

$\alpha_s$  is expanded to some order  $n$  in the cross-section calculation and as well in estimating the PDFs. To account for missing higher orders corrections of these expansions scale variations of the renormalization and factorization scales are performed pairwise  $\{\mu_r, \mu_f\} \times \{0.5, 0.5\}, \{1, 0.5\}, \{0.5, 1\}, \{1, 1\}, \{2, 1\}, \{1, 2\}, \{2, 2\}$ . For the cross-section calculation this accounts essentially for the term  $\mathcal{O}(\alpha_s^{n+1})$  in

equation 1.4.2. The envelope that gives the largest variation is taken as the scale uncertainty.

### PDF Uncertainties

PDFs need to be deduced from experiment and thus come by themselves with experimental uncertainties. Further uncertainties arise from the functional forms assumed for the PDFs.

### $\alpha_s$ Uncertainties

$\alpha_s$  is also experimentally deduced at the scale of the  $Z$  mass which is subject to uncertainties. In all perturbative calculations it is truncated at some order that needs to be accounted for.

The uncertainties on  $\alpha_s$  and the PDFs are both estimated by varying  $\alpha_s$ . Even though there correlation is not strong they are usually applied combined [5].

#### 1.4.1 Uncertainty on HH cross section

The cross-section calculation for the vector-boson fusion (VBF) Higgs pair production process has associated uncertainties for the scale variations  $^{+0.03\%}_{-0.04\%}$  and the combined PDF+ $\alpha_s$  uncertainty is  $\pm 2.1\%$  [7].

#### 1.4.2 Uncertainty on Acceptance

Theoretical uncertainties on the final acceptance are evaluated on MC simulations for scale variations and PDFs +  $\alpha_s$  **TODO, although shouldnt matter...**

#### 1.4.3 Parton Shower

Uncertainties related to the parton showering are estimated using different models from PYTHIA 8 and HERWIG 7. The largest deviations from the nominal are used as uncertainties on the Higgs pair process. **TODO**

### 1.4.4 Branching Ratio Uncertainty

The error estimate for the branching ratio takes into account theoretical uncertainties (THU) and parametric uncertainties (PU) that are included in the Standard Model (SM) calculations. The theoretical uncertainties mainly considers missing higher orders while for the parameters  $p$  the four leading non-negligible contributions of  $p = \alpha_s, m_c, m_b, m_t$  are considered.

Parametric uncertainties are Gaussian errors and are added in quadrature which ensures unity in the Branching Ratio calculation. Theoretical uncertainties in turn are not Gaussian and would lead to underestimated errors and are therefore added linearly [7]. By assuming a Higgs mass of 125 GeV and considering that there are two Higgs decaying to two  $b$ -quarks the error on the branching is

$$\Delta\text{BR} = 2 \times \left( \Delta\text{BR}(\text{THU}) + \sqrt{\sum_p \Delta\text{BR}(\text{PU}_p)^2} \right) = {}^{+3.4\%}_{-3.5\%}. \quad (1.4.3)$$

## 1.5 Statistical Uncertainties

As discussed in the chapter on statistics 2 the bin content for histograms in this work follows a Poisson distribution. Therefore the standard error for  $N$  events is the square root of the variance  $\sigma = \sqrt{\text{Var}} = \sqrt{N}$ . Since histograms are filled weighted  $\sum_i w_i N_i$  this needs to be taken into account. By making use of the additive property and invariance with respect to constants of the variance a bin filled with weights  $w_i$  can be written as

$$\begin{aligned} \sigma_{\text{stat}}^2 &= \text{Var}_{\text{bin}} \left( \sum_i w_i \right) = \underbrace{\sum_i \text{Var}(w_i \times 1 \text{ event})}_{\text{Var}(i+j)=\text{Var}(i)+\text{Var}(j)} = \underbrace{\sum_i w_i^2 \text{Var}(1 \text{ event})}_{\text{Var}(aX)=a^2\text{Var}(X)} \quad (1.5.1) \\ &= \sum_i w_i^2 \sqrt{(1 \text{ event})}, \end{aligned}$$

so that the statistical error reads

$$\sigma_{\text{stat}}^{\text{bin}} = \sqrt{\sum_i w_i^2}. \quad (1.5.2)$$

## 1.6 Background Derivation Uncertainties

The Quantum Chromodynamics (QCD) background is estimated with the ABCD method from the control region as detailed in section ???. The uncertainties are assessed through error propagation of the statistical uncertainty meaning the statistical errors of the event yields used to retrieve the weight factor result in an uncertainty for the weight factor  $\Delta w_{\text{CR}} = 0.0\%$ . To estimate a bin-wise statistical uncertainty of the NN score histogram the ABCD procedure is applied in the VR by also propagating the error  $\Delta w_{\text{CR}}$  of the applied weight factor.

# Chapter 2

## Statistics

Every scientific investigation starts with a hypothesis that is to be tested empirically. The main objective is to evaluate if the proposed hypothesis agrees or disagrees with observed data, to either accept or reject it against the null-hypothesis which represents a baseline scenario where only known phenomena are presumed to occur.

A key metric that quantifies this is the p-value that arises within hypothesis testing. Test results of an experiment follow some probability density function. Assuming some hypothesis, the p-value is the integrated probability for test results compatible with this hypothesis and ergo measuring the compatibility of the observation to the assumption. In other words if the experiment were to be repeated it gives the probability that the result favors the proposed hypothesis.

In the field of high energy physics a framework has been developed specifically for this task. This section begins to lay out the mathematical fundamentals of the approach and explains its implementation in PYHF [8, 9]. The following is based on [8, 10, 11].

### 2.1 Profile Likelihood Ratio

The statistical model needs to reflect the compatibility of predictions with the observed collision events. This can be quantified by a likelihood  $L(\boldsymbol{x}|\boldsymbol{\phi})$  which is a probability for an observation  $\boldsymbol{x}$  under a given set of parameters  $\boldsymbol{\phi}$  that govern



the predictions. Given that this is a counting experiment bins of a histogram  $\mathbf{h} = (h_1, \dots, h_N)$  are the main tool of analysis.

The observation can be subdivided  $\mathbf{x} = (\mathbf{n}, \mathbf{a})$  into observable histograms  $\mathbf{n}$  and auxiliary measurements. Observable histograms could be the invariant mass of a particle on the other hand auxiliary measurement histograms  $\mathbf{a}$  can be any additional observable that assist in constraining the model. For instance they can be a measurement of a kinematic variable in a phase space region where only background is expected. It should be noted that these auxiliary measurements are not equivalent to the inclusion of uncertainties into the model. The treatment of uncertainties is addressed separately in section 2.4.

Another useful splitting for the set of parameters  $\boldsymbol{\phi} = (\boldsymbol{\psi}, \boldsymbol{\Theta})$  into so-called parameters of interest  $\boldsymbol{\psi}$  and nuisance parameters  $\boldsymbol{\Theta}$ . For this section only one parameter of interest is considered, the signal strength  $\mu$ .

The bin contents can then be expressed in terms of the amount of signal  $s_i(\boldsymbol{\Theta})$  and background  $b_i(\boldsymbol{\Theta})$  in bin  $i$  that depend on the nuisance parameters. The prediction (expectation value) of the histogram bins of the observable  $n_i$  can then be expressed as

$$\langle n_i(\mu, \boldsymbol{\Theta}) \rangle = \mu s_i(\boldsymbol{\Theta}) + b_i(\boldsymbol{\Theta}). \quad (2.1.1)$$

Similarly for auxiliary measurement bins  $a_i$  their expectation value are calculable from some function  $u_i(\boldsymbol{\Theta})$  modeling some observable and is also dependent on the nuisance parameters

$$\langle a_i(\boldsymbol{\Theta}) \rangle = u_i(\boldsymbol{\Theta}). \quad (2.1.2)$$

Since this is a counting experiment in which events occur at a constant mean rate and independently of time each bin follows a Poisson distribution

$$P(r, k) = \frac{r^k e^{-r}}{k!}. \quad (2.1.3)$$

$r$  is the expected rate of occurrences which translates as the prediction whereas  $k$  are the actual measured occurrences. A likelihood can then be constructed from a

product of Poisson probabilities

$$L(\mu, \Theta) = \prod_{j=1}^N \frac{(\mu s_j(\Theta) + b_j(\Theta))^{n_j}}{n_j!} e^{-(\mu s_j(\Theta) + b_j(\Theta))} \prod_{k=1}^M \frac{u_k(\Theta)^{a_k}}{a_k!} e^{-u_k(\Theta)}. \quad (2.1.4)$$

The last product can also be thought of penalizing the likelihood if e.g. an auxiliary measurement displays a very improbable value for some quantity. To test for a hypothesized value of  $\mu$ , the best choice according to the Neyman-Pearson lemma [11], is the profile likelihood ratio that reduces the dependence to the parameter(s) of interest

$$\lambda(\mu) = \frac{L(\mu, \hat{\Theta})}{L(\hat{\mu}, \hat{\Theta})}. \quad (2.1.5)$$

The denominator is the unconditional maximum likelihood estimate so that  $\hat{\mu}$  and  $\hat{\Theta}$  both are free to vary to maximize  $L$ , whereas the numerator is the found maximum likelihood conditioned on some chosen  $\mu$  and the set of nuisance parameters  $\hat{\Theta}$  that maximize the likelihood for that particular  $\mu$ . This definition gives  $0 \leq \lambda \leq 1$  where  $\lambda = 1$  corresponds to perfect agreement of the hypothesized value of  $\mu$  to the model.

## 2.2 Test Statistic and p-value

To test for alternative hypotheses it is useful to transform the profile likelihood into a test statistic

$$t(\mu) = -2 \ln \lambda(\mu). \quad (2.2.1)$$

This translates to  $t \rightarrow 0$  as increasing agreement and  $t \rightarrow \infty$  as decreasing agreement to the model. A right-tail p-value can then be calculated from the probability density function of the test statistic:  $\text{PDF}(t) = f(t|\mu)$

$$p = \int_{t_{\text{obs}}}^{\infty} f(t|\mu) dt \quad (2.2.2)$$

$t_{\text{obs}}$  is the test statistic  $t$  evaluated at the observed data which means replacing the predictions in the likelihood of the numerator of equation 2.1.5 with the values observed in data. Similar to the PDF of a standard normal distribution the PDF

in this context quantifies how probable a particular value of the test statistic  $t$  is under a fixed value of the signal strength. This essentially measures how frequently a particular value of  $t$  occurs in comparison to all other possible values that  $t$  can take.

To calculate p-values the integral of equation 2.2.2 must be solved. The test statistic's specific form is useful because it allows for approximations of  $f(t|\mu)$  [10]. Let  $f(t|\mu')$  be the probability distribution for the true strength parameter  $\mu'$ . Wald [12] demonstrated that for a single parameter of interest the test statistic is equivalent to a normalized sum of squared distances between the tested parameter  $\mu$  and its maximum likelihood estimate  $\hat{\mu}$

$$t(\mu) = -2 \ln \lambda(\mu) = \left( \frac{\mu - \hat{\mu}}{\sigma_{\hat{\mu}}} \right)^2 + \mathcal{O}\left(\frac{1}{\sqrt{N}}\right). \quad (2.2.3)$$

The maximum likelihood estimate  $\hat{\mu}$  is in the large sample limit normally distributed around their true value  $\mu'$  with standard deviation  $\sigma_{\hat{\mu}}$ . This is the definition of a  $\chi$ -squared distribution with one degree of freedom. It can be shown that [10] the PDF of  $t$  is asymptotically follows

$$f(t|\mu) = \frac{1}{2\sqrt{t}} \frac{1}{\sqrt{2\pi}} \left[ \exp\left(-\frac{1}{2}(\sqrt{t} + \sqrt{\Lambda_\mu})\right) + \exp\left(-\frac{1}{2}(\sqrt{t} - \sqrt{\Lambda_\mu})\right) \right], \quad (2.2.4)$$

with the non-centrality parameter as the normalized distance between the tested  $\mu$  and true parameter of interest  $\mu'$

$$\Lambda_\mu = \frac{(\mu - \mu')^2}{\sigma^2}. \quad (2.2.5)$$

Figure 2.1 illustrates these steps. Being able to calculate p-values allows to state how likely it is that the proposed hypothesis is reflected by the observed data. In other words, the p-value represents the probability, how incompatible the proposed hypothesis or prediction is with the observation.

In the scientific community a p-value of 0.05 is commonly accepted as significant. Though particle physicists only claim discovery of a new phenomenon for  $p < 2.87 \times 10^{-7}$  corresponding to 5 standard deviations of the standard normal distribution and exclude hypotheses if the p-value is not below 2 standard deviations of the

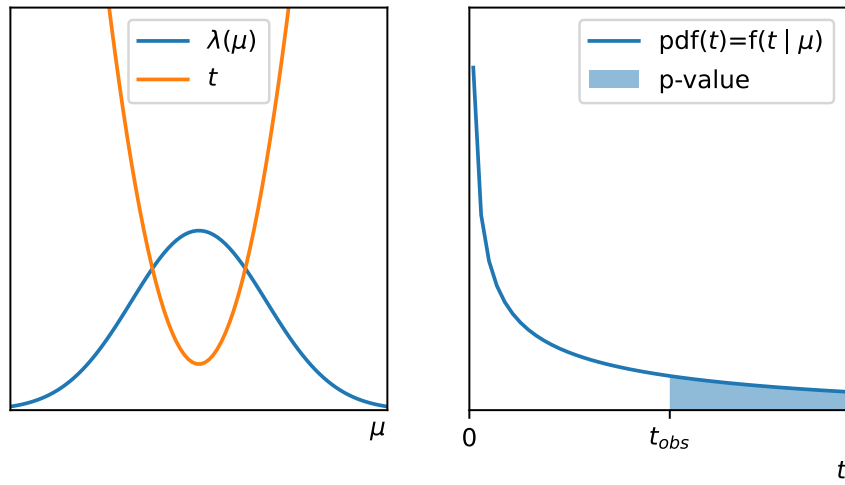


**Figure 2.1:** A sketch to follow the steps to calculate p-values. (**left**) The profile likelihood (■) has essentially some hill-like form with a maximum at  $\lambda(\hat{\mu}, \hat{\Theta})$ . The test statistic  $t$  (■) is calculated as  $-2\ln(\lambda)$ . (**right**) For one parameter of interest in the large sample limit  $f(t|\mu)$  from equation 2.2.4 follows a non-central chi-squared distribution with one degree of freedom. The blue shaded area under the PDFs is a right hand sided p-value.

standard normal distribution  $p \lesssim 0.05$ . A key consideration is that  $t$  can assume negative values for  $\mu$  which might be non-physical depending on the context. This is handled by cutting off the test statistic for undesired behavior. An example of an adjusted test statistic for setting upper limits is

$$q_\mu = \begin{cases} -2 \ln \lambda(\mu) & \hat{\mu} \leq \mu \\ 0 & \hat{\mu} > \mu \end{cases}. \quad (2.2.6)$$

Here if a tested signal strength  $\mu$  is not larger than the maximum estimate it would not be regarded as less compatible and is therefore set to zero. [10] covers other cases and pdf approximations for various scenarios.

## 2.3 The $CL_s$ value

Particle physicists typically concentrate on two key aspects when performing statistical tests to discover new phenomena: the accurate modeling of known backgrounds and whether there is evidence in the observations for a new phenomenon. This involves assessing two distinct hypotheses: a background only ( $b$ ) and one that involves signal and background ( $s + b$ ). Each will result in a p-value of their own.

For example, a p-value of  $p_b = 0$  would indicate a perfect modeling of the background model reflected in observational data, meaning that known phenomena have been accurately accounted for. Conversely, a p-value of  $p_{s+b} < 0.05$  might signal the presence of new phenomena, such as previously undiscovered physics.

To synthesize these two aspects into a unified metric particle physicists developed a pseudo Confidence Level/p-value referred to as  $CL_s$ . This measure not only considers the potential presence of new phenomena but also the accuracy of the background modeling.

$$CL_s = \frac{p_{s+b}}{1 - p_b} = \frac{\int_{t_{\text{obs}}}^{\infty} f(t_{s+b}|\mu) dt}{1 - \int_{t_{\text{obs}}}^{\infty} f(t_b|\mu) dt}. \quad (2.3.1)$$

The numerator represents the p-value for the alternative hypothesis while the denominator p-value penalizes the  $CL_s$  based on how compatible the background model is with the observational data. This concept can also be understood visually

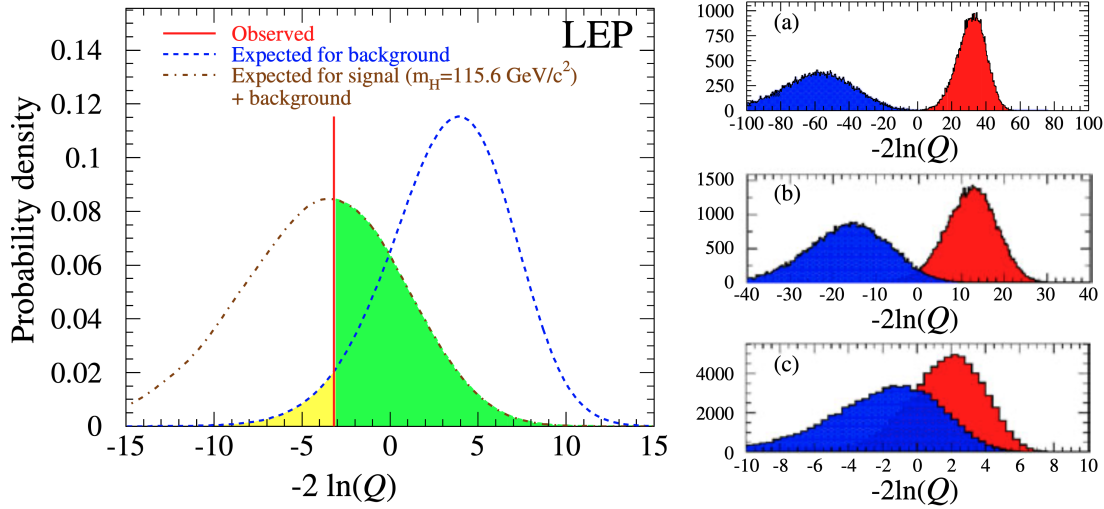


**Figure 2.2:** Probability density functions of test statistics from a Higgs search at LEP illustrating the calculation of p-values ( $\lambda$  becomes  $Q$ ). **(left)** The PDFs's of the test statistic  $f(t|\mu)$  of the signal + background (—) and background (---) only hypotheses. The p-value is calculated by integration from  $t_{\text{obs}}$  (the red observed line (—)) to infinity (see eq. 2.2.2). The green shaded area (■) corresponds to  $p_{s+b}$  whereas the yellow area (■) corresponds to  $1 - p_b$  since the integral over one whole PDFs is 1. **(right)** Degradation of search sensitivity from (a) to (c). Note that the colors of the PDFs's change here to signal + background (■) and background only (■). For example putting the observation ( $t_{\text{obs}}$ ) on the x-axis at 0 in these plots, one would get for plot (a)  $p_b \approx 1$  and  $p_{s+b} \approx 0$  resulting in a  $\text{CL}_s \approx 0$ , whereas with increasing overlap the  $\text{CL}_s$  value increases and the sensitivity decreases. Adopted from [13].

from the first figure of the paper that introduced the  $\text{CL}_s$  quantity [13] and is explained here in figure 2.2.

## 2.4 HistFactory

A widely-used model for constructing likelihoods as discussed in section 2.1 is known as HistFactory [14]. This model is implemented in the PYHF toolkit [8] and the following section is primarily based on the introduction to HistFactory found in the PYHF documentation. HistFactory simplifies the process of building a likelihood by breaking it down into several fundamental components. To understand this it is

helpful to consider a different categorization of the model parameters  $\phi$

$$L(\mathbf{x}|\phi) = \underbrace{L(\mathbf{x}|\underbrace{\psi}_{\text{parameters of interest}}, \underbrace{\theta}_{\text{nuisance parameters}})}_{\text{parameters of interest}} = L(\mathbf{x}|\underbrace{\eta}_{\text{free}}, \underbrace{\chi}_{\text{constrained}}), \quad (2.4.1)$$

Free parameters  $\eta$  are free to choose in the model and can be for example a cross-section of a process. Constrained parameters  $\chi$  are used to incorporate uncertainties into the likelihood to constrain it. Further there might be several histograms of an observable, for example measured in orthogonal kinematic regions, that are called channels  $c$ . Bins have the index  $b$  here and constraint terms are denoted  $c_\chi$ . The likelihood can thus be described by

$$L(\mathbf{n}, \mathbf{a} | \eta, \chi) = \underbrace{\prod_{c \in \text{channels}} \prod_{b \in \text{bins}_c} \text{Pois}(\underbrace{n_{cb}}_{\text{observed}} | \underbrace{\nu_{cb}(\eta, \chi)}_{\text{predicted}})}_{\text{Simultaneous measurement of multiple channels}} \underbrace{\prod_{\chi \in \chi} c_\chi(a_\chi | \chi)}_{\text{constraint terms for auxiliary measurements}}. \quad (2.4.2)$$

$\mathbf{n}$  and  $\mathbf{a}$  are the observations auxiliary measurement histograms as defined in section 2.1. The  $n_{cb}$  is the observed bin content and  $\nu_{cb}(\eta, \chi)$  the predicted bin content.  $c_\chi(a_\chi | \chi)$  are functions that calculate a probabilistic impact to the likelihood  $L$  of uncertainties  $a_\chi$  to constrain the parameter  $\chi$  and are discussed in detail section 2.6.

The prediction is a sum of nominal bin counts<sup>1</sup>  $\nu_{scb}^0$  over all samples  $s$  (e.g.  $t\bar{t}$ , multijet-background, etc.). These nominal bin counts are subject to uncertainties. Therefore the bin content can be varied within the bounds of these uncertainties. However the effect of this modification to the likelihood must be taken into account which is through the constraint terms. These penalize the likelihood proportional to the modification. Modifiers are discussed in detail in section 2.5. They enter the likelihood through linear modeling of the nominal bin content  $\nu_{scb}^0$  with

---

<sup>1</sup>also called rates, like in the definition of a Poisson distribution

multiplicative  $\kappa_{scb}$  and additive modifiers  $\Delta_{scb}$

$$\nu_{cb}(\boldsymbol{\eta}, \boldsymbol{\chi}) = \sum_{s \in \text{samples}} \nu_{scb}(\boldsymbol{\eta}, \boldsymbol{\chi}) \quad (2.4.3)$$

$$= \sum_{s \in \text{samples}} \underbrace{\left( \prod_{\kappa \in \boldsymbol{\kappa}} \kappa_{scb}(\boldsymbol{\eta}, \boldsymbol{\chi}) \right)}_{\text{multiplicative modifiers}} \left( \nu_{scb}^0 + \underbrace{\sum_{\Delta \in \boldsymbol{\Delta}} \Delta_{scb}(\boldsymbol{\eta}, \boldsymbol{\chi})}_{\text{additive modifiers}} \right). \quad (2.4.4)$$

The usefulness of this approach becomes clear when considering one uncertainty  $a_\chi$  on a nominal bin count estimate  $\nu_{scb}^0$ . The main goal remains to maximize the overall likelihood  $L$ . This can be achieved via maximizing the Poisson probability (blue part in equation 2.4.2) and at the same time keeping the constraint term (red part in equation 2.4.2) large. It is illustrative to consider one nuisance parameter  $\chi$  as a multiplicative modifier  $\kappa_{scb} = \chi$  on  $\nu_{scb}^0$ . An optimum can be found by modifying the prediction to move closer to the observed value (blue part in equation 2.4.2) while at the same time keeping the constraint term  $c_\kappa(\kappa)$  (red part in equation 2.4.2) controlled by the same  $\chi$  at values where the penalization of the likelihood stays insignificant. This works well for example when  $\kappa$  has a very large uncertainty rendering the constraint term's influence on the likelihood relatively small.

## 2.5 The Modifiers

In HistFactory there are by convention four types  $\{\lambda, \mu, \gamma, \alpha\}$  of such multiplicative rate modifiers that are explained in this section. There are **free rate modifiers** for the luminosity  $\lambda$  and signal strength  $\mu$  that affect all bins equally

$$\nu_{scb}(\mu) = \mu \nu_{scb}^0. \quad (2.5.1)$$

These are bin-independent normalization factors and preserve the shape of the histogram. Further there are **bin-wise modifiers**  $\gamma_b$  (uncorrelated shape)

$$\nu_{scb}(\gamma_b) = \gamma_b \nu_{scb}^0. \quad (2.5.2)$$



These are useful for example to include uncertainties of a per bin data-driven background estimate. This type without a constraint term is not of much use as if there is only one sample or channel, the fit would always match the data perfectly. In addition there exist **interpolation parameters**  $\alpha$  (shape factors) that enter the modeling through an interpolation function  $\eta$  instead of being the factor itself. They exist in multiplicative versions

$$\nu_{scb}(\alpha) = \eta(\alpha)\nu_{scb}^0, \quad (2.5.3)$$

and additive versions

$$\nu_{scb}(\alpha) = \nu_{scb}^0 + \eta(\alpha). \quad (2.5.4)$$

This is useful to include systematic uncertainties. Typically they are known for one standard deviation of a bin count  $\eta_{-1} = \nu_{scb}^{1\text{down}}$  and  $\eta_1 = \nu_{scb}^{1\text{up}}$  to the nominal value  $\nu_{scb}^0$ . These are then used to construct interpolation functions that modify the nominal value controlled by the nuisance parameter that also controls the constraint term  $c_\alpha$  which is further explained in section 2.6. Thus one parameter controls the modification and constraint at a time.

In HistFactory there exists four of such interpolation functions. For those exist an identity operator

$$\eta_0 = \eta(\alpha = 0) = \begin{cases} 1, & \text{multiplicative modifier, } (\kappa) \\ 0, & \text{additive modifier, } (\lambda). \end{cases} \quad (2.5.5)$$

One example of these interpolation functions that scales the bin count linearly over the known deviations  $\eta_{-1} = \nu_{scb}^{1\text{down}}$  and  $\eta_1 = \nu_{scb}^{1\text{up}}$  is

$$\eta_{\text{linear}}(\alpha) = \begin{cases} \alpha(\eta_0 - \eta_1), & \alpha > 0 \\ \alpha(\eta_0 - \eta_{-1}), & \alpha < 0 \end{cases} \quad (2.5.6)$$

This is illustrated in fig. 2.3(a). For the other ones see e.g. [15]. It is noted that  $\alpha$  is the nuisance parameter and not the function  $\eta(\alpha)$  and there is an associated constraint term  $c_\alpha$  to each  $\alpha$ .

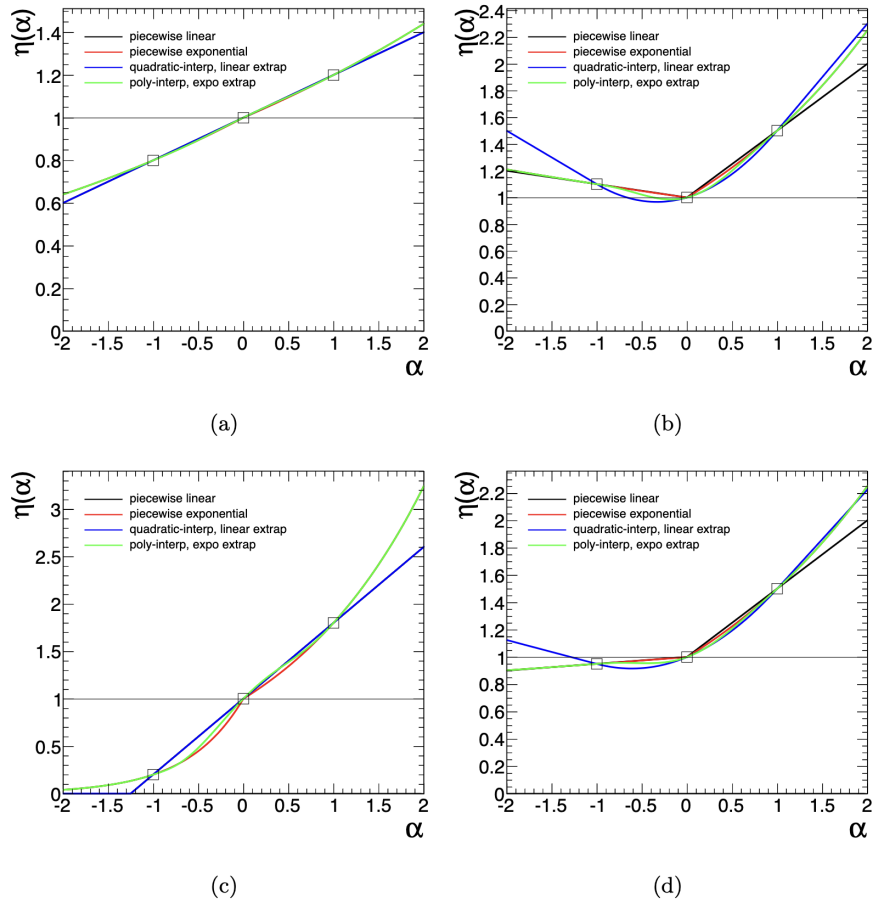


**Figure 2.3:** The four interpolation functions  $\eta(\alpha)$  for different up and down standard deviation values. For example in (a) the bin count will be scaled with a factor of 0.8 for an  $\alpha = -1$  (1.2 for an  $\alpha = 1$ ). From [14].

## 2.6 The constraint terms

Uncertainties are modeled either Gaussian or Poissonian. The Gaussian uncertainty implementation is straightforward as the standard deviation  $\sigma$  appears in the definition of the Gaussian with mean  $\mu$

$$\text{Gaus}(\mu|x, \sigma) = \frac{1}{\sigma\sqrt{2\pi}} e^{-\frac{1}{2}\left(\frac{x-\mu}{\sigma}\right)^2}. \quad (2.6.1)$$

So that the likelihood for a Gaussian uncertainty is constrained by a Gaussian scaled to one standard deviation controlled by the nuisance parameter  $\alpha$ :  $\text{Gauss}(\alpha|a, \sigma = 1)$ .

Similar to the Gaussian uncertainty for an uncertainty that is Poissonian distributed

$$\text{Pois}(r|\rho) = \frac{\rho^r e^{-\rho}}{r!}. \quad (2.6.2)$$

the nuisance parameter for a multiplicative factor  $\kappa_{scb} = \gamma$  in equation 2.4.4 should control the Poisson constraint term such that the uncertainty  $\sigma$  is reflected by the variance of the Poisson  $\text{Var}(\text{Pois}) = \rho = \sigma^2$ . This is achieved by scaling the distribution with a factor  $f$  which is then solved for the one with the desired uncertainty by evaluating it at the nominal value of the multiplicative modifier  $\gamma_0 = 1$

$$\text{Var} [\text{Pois}(r = f\gamma_0|\rho = f\gamma)] = \rho = f\gamma \stackrel{\gamma=\gamma_0}{=} f\gamma_0 = (f\sigma)^2 \rightarrow f = (1/\sigma^2). \quad (2.6.3)$$

Thus a Poissonian constraint term for a multiplicative modifier  $\gamma$  reads  $\text{Pois}(r = \sigma^{-2}|\rho = \sigma^{-2}\gamma)$ . This completes the necessities for the HistFactory model. The different types of modifiers and their constraint terms are summarized in table 2.1.

**Table 2.1:** Modifiers and constraint terms used in HistFactory implemented by PYHF. Note that the interpolation functions are called  $f_p$  and  $g_p$  here instead of  $\eta$  as chosen in the full text. Adopted from [8]

Description	Modification	Constraint Term $c_\chi$	$c_\chi$ input
Uncorrelated Shape	$\kappa_{scb}(\gamma_b) = \gamma_b$	$\prod_b \text{Pois}(r_b = \sigma_b^{-2}   \rho_b = \sigma_b^{-2} \gamma_b)$	$\sigma_b$
Correlated Shape	$\Delta_{scb}(\alpha) = f_p(\alpha   \Delta_{scb, \alpha=-1}, \Delta_{scb, \alpha=1})$	$\text{Gaus}(a = 0   \alpha, \sigma = 1)$	$\Delta_{scb, \alpha=\pm 1}$
Normalisation Unc.	$\kappa_{scb}(\alpha) = g_p(\alpha   \kappa_{scb, \alpha=-1}, \kappa_{scb, \alpha=1})$	$\text{Gaus}(a = 0   \alpha, \sigma = 1)$	$\kappa_{scb, \alpha=\pm 1}$
MC Stat. Uncertainty	$\kappa_{scb}(\gamma_b) = \gamma_b$	$\prod_b \text{Gaus}(a_{\gamma_b} = 1   \gamma_b, \delta_b)$	$\delta_b^2 = \sum_s \delta_{sb}^2$
Luminosity	$\kappa_{scb}(\lambda) = \lambda$	$\text{Gaus}(l = \lambda_0   \lambda, \sigma_\lambda)$	$\lambda_0, \sigma_\lambda$
Normalisation	$\kappa_{scb}(\mu_b) = \mu_b$		
Data-driven Shape	$\kappa_{scb}(\gamma_b) = \gamma_b$		

---

# Part I

## Results

## Chapter 3

### $HH \rightarrow 4b$ Results

#### 3.1 Background validation

$$\frac{N(\text{CR}, 2\text{Xbb})}{N(\text{CR}, 1\text{Xbb})} = 0.0 \pm 0.0.$$

---

# Appendices

# Appendix A

## Acronyms

**CERN** Organisation européenne pour la recherche nucléaire

**ATLAS** A Toroidal LHC Apparatus

**SM** Standard Model

**QFT** Quantum Field Theory

**QCD** Quantum Chromodynamics

**QED** Quantum Electrodynamics

**EW** Electroweak

**EWSB** Electroweak Symmetry Breaking

**VEV** Vacuum Expectation Value

**CKM** Cabibbo-Kobayashi-Maskawa

**EM** electromagnetic

**IP** impact parameter of tracks

**ML** Machine Learning

**neos** neural end-to-end-optimized summary statistics



**HEP** High Energy Physics

**LHC** Large Hadron Collider

**HL-LHC** High Luminosity LHC

**ID** Inner Detector

**SCT** semiconductor tracker

**TRT** transition radiation tracker

**IBL** insertable *b*-layer

**HLT** high level trigger

**L1** Level-1

**PFO** Particle Flow Object

**TCC** Track CaloCluster

**UFO** Unified Flow Object

**JES** Jet Energy Scale

**JER** Jet Energy Resolution

**JMR** Jet Mass Resolution

**GGF** gluon-gluon fusion

**VBF** vector-boson fusion

**NNLO** next-to-next-to-leading order

**N<sup>3</sup>LO** next-to-next-to-next-to-leading order

**SR** Signal Region

**VR** Validation Region

**CR** Control Region

**KDE** Kernel Density Estimation

**bKDE** binned Kernel Density Estimation

**MC** Monte Carlo

**PDF** Parton Density Function

**PV** primary vertex

**JVT** jet vertex tagger

**NN** Neural Network

**ANN** Artificial Neural Network

**WP** working point

**VR** variable radius

# Appendix B

## Cutflow

TODO, also fine like that?

Selection	Event	Fraction [%]	Total Fraction [%]
Initial	16854036422.000		
Preselections (MNT + Jet Cleaning)	670573995.000	100.000	100.000
PassTrigBoosted	63944638.000	9.536	9.536
PassTwoFatJets	57510800.000	89.938	8.576
PassTwoHbbJets	12875.000	0.0223	<0.001
PassVBFJets	5762.000	44.753	<0.001
PassFatJetPt	3902.000	67.720	<0.001
PassVBFCut	314.000	8.047	<0.001

**Table B.1:** Cut-flow table for data before signal region cut

Selection	Event	Fraction [%]	Total Fraction [%]
Initial	1475.226		
Preselections (MNT + Jet Cleaning)	547.960	100.000	100.000
PassTrigBoosted	20.926	3.819	3.819
PassTwoFatJets	14.141	67.576	2.581
PassTwoHbbJets	5.353	37.852	0.977
PassVBFJets	2.243	41.903	0.409
PassFatJetPt	1.408	62.793	0.257
PassVBFCut	0.148	10.539	0.027
PassSR	0.097	65.484	0.018
OverlapRemoval	0.059	61.200	0.011

**Table B.2:** Cut-flow table for DSID = 600463



# Bibliography

- [1] ATLAS Collaboration atlas. publications@ cern. ch, Georges Aad, B Abbott, DC Abbott, A Abed Abud, K Abeling, DK Abhayasinghe, SH Abidi, OS AbouZeid, NL Abraham, et al. Jet energy scale and resolution measured in proton–proton collisions at  $\sqrt{s} = 13$  tev with the atlas detector. *The European Physical Journal C*, 81(8):689, 2021. doi:10.48550/arXiv.2007.02645.
- [2] The ATLAS collaboration. In situ calibration of large-radius jet energy and mass in 13 tev proton–proton collisions with the atlas detector. *The European Physical Journal C*, 79(2):135, 2019. doi:10.1140/epjc/s10052-019-6632-8. URL <https://doi.org/10.1140/epjc/s10052-019-6632-8>.
- [3] ATLAS Collaboration. Measurement of the ATLAS Detector Jet Mass Response using Forward Folding with  $80 \text{ fb}^{-1}$  of  $\sqrt{s} = 13 \text{ TeV}$   $pp$  data. ATLAS-CONF-2020-022, 2020. URL <https://cds.cern.ch/record/2724442>.
- [4] ATLAS Collaboration. Efficiency corrections for a tagger for boosted  $H \rightarrow b\bar{b}$  decays in  $pp$  collisions at  $\sqrt{s} = 13 \text{ TeV}$  with the ATLAS detector. Technical report, CERN, Geneva, 2021. URL <https://cds.cern.ch/record/2777811>.
- [5] The ATLAS collaboration. Particle Modeling Group systematic uncertainty recipes. URL <https://twiki.cern.ch/twiki/bin/view/AtlasProtected/PmgSystematicUncertaintyRecipes>. Last accessed: 2023-11-29.
- [6] Francis Halzen, A Martin, and Leptons Quarks. An introductory course in modern particle physics. *John and Wiley*, 1984.

- [7] Daniel de Florian, D Fontes, J Quevillon, M Schumacher, FJ Llanes-Estrada, AV Gritsan, E Vryonidou, A Signer, P de Castro Manzano, D Pagani, et al. *arXiv: Handbook of LHC Higgs Cross Sections: 4. Deciphering the Nature of the Higgs Sector*. Number arXiv: 1610.07922. Cern, 2016.
- [8] Lukas Heinrich, Matthew Feickert, and Giordon Stark. pyhf: v0.7.2. URL <https://doi.org/10.5281/zenodo.1169739>. <https://github.com/scikit-hep/pyhf/releases/tag/v0.7.2>.
- [9] Lukas Heinrich, Matthew Feickert, Giordon Stark, and Kyle Cranmer. pyhf: pure-python implementation of histfactory statistical models. *Journal of Open Source Software*, 6(58):2823, 2021. doi:10.21105/joss.02823. URL <https://doi.org/10.21105/joss.02823>.
- [10] Glen Cowan, Kyle Cranmer, Eilam Gross, and Ofer Vitells. Asymptotic formulae for likelihood-based tests of new physics. *The European Physical Journal C*, 71:1–19, 2011.
- [11] Olaf Behnke, Kevin Kröninger, Grégory Schott, and Thomas Schörner-Sadenius. *Data analysis in high energy physics: a practical guide to statistical methods*. John Wiley & Sons, 2013.
- [12] Abraham Wald. Tests of statistical hypotheses concerning several parameters when the number of observations is large. *Transactions of the American Mathematical society*, 54(3):426–482, 1943.
- [13] Alexander L Read. Presentation of search results: the cls technique. *Journal of Physics G: Nuclear and Particle Physics*, 28(10):2693, 2002.
- [14] Kyle Cranmer, George Lewis, Lorenzo Moneta, Akira Shibata, and Wouter Verkerke. HistFactory: A tool for creating statistical models for use with RooFit and RooStats. Technical report, New York U., New York, 2012. URL <https://cds.cern.ch/record/1456844>.
- [15] Lukas Heinrich. *Searches for Supersymmetry, RECAST, and Contributions to Computational High Energy Physics*. PhD thesis, New York University, 2019.

### **Statutory Declaration - Eidesstattliche Erklärung**

I declare that I have authored this thesis independently, that I have not used other than the declared sources/ resources and that I have explicitly marked all materials which has been quoted either literally or by content form the used sources.

Hiermit erkläre ich, dass ich die vorliegende Arbeit selbstständig verfasst, andere als die angegebenen Quellen/Hilfsmittel nicht benutzt und die den benutzten Quellen wörtlich und inhaltlich entnommenen Stellen als solche kenntlich gemacht habe.

Berlin, 07.12.2023

---

Frederic Renner